Excited states of the saddle point equation of the Landau-Ginzburg-Wilson Hamiltonian with random temperature

X. T. Wu
Department of Physics, Beijing Normal University, Beijing 100875, China
(Received 17 February 2009; revised manuscript received 30 April 2009; published 26 May 2009)

The phase transition in quenched disordered systems is studied on the level of the saddle point solution. Two-dimensional saddle point equation of the Landau-Ginzburg-Wilson Hamiltonian with random temperature is numerically solved for the excited states. It is shown that the excited-state solutions can be described by the domain walls. The length of domain wall and the free energy increase due to the domain wall are calculated. On the level of the saddle point solution the partition function can be mapped to an Ising model approximately. The coupling between Ising spin is estimated. The phase transition is discussed according to this Ising model. It is found that there are two classes of phase transition: inhomogeneous and homogeneous. Different from the pure system, for the phase transition in disordered systems there are fluctuations on the level of saddle point solution.

DOI: 10.1103/PhysRevB.79.184208 PACS number(s): 05.70.Fh, 64.60.Bd

I. INTRODUCTION

The phase transition in quenched disordered systems has been studied for 40 years.[1] Although there have been a huge amount of works on this topic, there is a basic problem unsolved. That is the saddle point equation (SPE) of the Landau-Ginzburg-Wilson (LGW) Hamiltonian with random temperature. We study this problem in this paper. Based on the numerical result, a complete description of phase transition on the level of saddle point solution is given.

As we know, most of phase transitions can be described by certain LGW Hamiltonian.[2] The classical LGW is the prototype. The saddle point solution is the starting point of the field theoretical study on phase transition. For the pure system, it is simple and clear. However it has not been studied carefully for the disordered systems, although some experiments and intuitive theoretical discussions show that it should be nontrivial.

On one hand locally ordered regions (LOR) are discovered in the experiments. LOR is suggested as early as in 1977 by Ginzburg[3] theoretically. The physical picture is simple and clear: owing to the spatial fluctuation of the local transition temperature, "ferromagnetic islands" (locally ordered regions), which is also called Griffiths-type phase, may exist above the critical temperature. LOR is discovered in the magnetic phase transition in disordered systems.[4–6] The experiments on the superfluid transition of ^{4}He in porous media also revealed the localized Bose condensation above the global superfluid transition temperature.[7,8] In order to explain recent scanning tunnel microscope STM experiments, an inhomogeneous gapped superconductor with superconducting islands and metallic regions is proposed.[9] The existence of ferromagnetic region in the paraphase is discovered.[10]

On the other hand, it is pointed out that there may exist many local minima solutions for the SPE above the critical temperature.[11,12] Conventional renormalization group (RG) considerations assume that the solution of SPE is zero above the critical temperature.[13–16] In recent years the replica symmetry breaking (RSB) is proposed to take LOR into account. The RG with RSB has been investigated intensively.[11,17–19] In addition a percolative scenario of LOR is also proposed for the phase transition in disordered systems.[12] The famous Harris' criterion[15] is questioned in this percolative scenario. However in these theoretical studies, the saddle point solution is only qualitatively discussed and its detailed properties are absent.

Some works on SPE of LGW Hamiltonian with random temperature has been carried out.[20–22] The numerical solutions show LOR explicitly. However these solutions are only concerned with the ground state rather than the excited states. From a qualitative discussion, one knows that the nature of the phase transition is determined by the excited states.

In this paper, we shall study the excited-state solutions of SPE with random temperature. The two-dimensional SPE with random temperature is solved numerically. After getting the excited-state solutions, we calculate the length of domain wall and its free-energy increase. From these results, we can estimate the degeneracy of the excited states. Then the phase transition on the level of saddle point solution is discussed.

The paper is arranged as follows. In Sec. II, the model with random temperature is introduced. In Secs. III and IV, as a warm-up, the domain wall around a round well and excited states on a regular well lattice are studied. The excited states of SPE with random temperature are discussed in Sec. V. The phase transition is discussed on the level of saddle point solution in Sec. VI. Section VII is discussion and summary.

II. MODEL OF RANDOM TEMPERATURE

The LGW Hamiltonian with random temperature reads

$$H = \int d\mathbf{r}\left\{\frac{1}{2}|\nabla\phi(\mathbf{r})|^2 + \frac{1}{2}t(\mathbf{r})\phi^2(\mathbf{r}) + \frac{g}{4}\phi^4(\mathbf{r})\right\}, \quad (1)$$

where $t(\mathbf{r})=t+\tilde{t}(\mathbf{r})$ and $t,\tilde{t}(\mathbf{r})$ are the average reduced temperature and the random part caused by the disorder, respectively. The system is modeled as a lattice with cell volume being l^d. In the ith cell, it has $\tilde{t}(\mathbf{r})=\tilde{t}_i$, and $\tilde{t}_i$ is a random number and distributed in the Gaussian form

$$p(\{\tilde{t}_i\}) = \frac{1}{\Delta_0\sqrt{2\pi}}\exp\left(-\frac{\tilde{t}_i^2}{2\Delta_0^2}\right). \quad (2)$$

The distribution width of the random temperature Δ_0 is called the disorder strength. The cell size l is the correlation length of disorder.[20]

After we get a saddle point solution, we need to calculate its free energy. Substituting SPE into Eq. (1), one gets[11]

$$F_i = H(\{\phi_i\}) = -\int d\mathbf{r}\frac{g}{4}\phi_i^4(\mathbf{r}), \quad (3)$$

where $\phi_i(\mathbf{r})$ is the ith solution of SPE. For the disordered systems, there are a lot excited states, which will determine the phase transition. On the saddle point level, where the fluctuation around the saddle point solution is ignored, the partition function is given by

$$Z = \sum_i e^{-F_i}. \quad (4)$$

Introducing the following transformations:

$$H' = gl^{4-d}H, \quad \mathbf{r}' = \frac{\mathbf{r}}{l},$$

$$t'(\mathbf{r}) = l^2 t(\mathbf{r}), \quad \phi'(\mathbf{r}) = l\sqrt{g}\phi(\mathbf{r}), \quad (5)$$

then the SPE is given by

$$-\nabla'^2\phi'(\mathbf{r}') + [t'(\mathbf{r}')]\phi'(\mathbf{r}') + \phi'^3(\mathbf{r}') = 0, \quad (6)$$

where the probability distribution of $\tilde{t}'$ is still a Gaussian one like Eq. (2) with an effective disorder strength

$$\Delta \equiv l^2\Delta_0. \quad (7)$$

From Eq. (3), we get the free-energy transformation for the ith state

$$F_i' = gl^{4-d}F_i, \quad (8)$$

where d is the spatial dimension. Thus one can solve the above SPE, and get the solution of equation with arbitrary l, g through transformations (5)–(8). Three original parameters g, l, Δ_0 are transformed to be 1, 1, $l^2\Delta_0$, respectively. Therefore there is only one concerned parameter, i.e., the reduced disorder strength $\Delta = l^2\Delta_0$.

Generally for the temperature t and disorder strength Δ are much smaller than unity. Since the disorder correlation length l can be larger than 1, therefore the temperature $t' = l^2 t$ and reduced disorder strength $\Delta = l^2\Delta_0$ can be much larger than 1.

In the following we omit the superscript "quotation mark" of the reduced variables "$t', \mathbf{r}', \phi'$" in Eq. (6). It is assumed that $g=1$, $l=1$ if there is no special statement.

III. DOMAIN WALL AROUND A ROUND WELL

In a pure two-dimensional system, the temperature in Eq. (6) is a constant, i.e., $t(\mathbf{r}) = t$. Beside the ground-state solution $\phi_0 = \pm\sqrt{-t}$, there are excited-state solutions

$$\phi_e(x) = \sqrt{-t}\tanh[\sqrt{-t/2}x], \quad (9)$$

assuming variation in only x direction. For these excited-state solutions, there are two phases separated by an interface, where $\phi_e = 0$. The interface is called domain wall. Here the domain wall is a straight line. The free energy of excited-state solution is higher than that of ground sate. We call their difference free-energy increase. Substituting the above solution into the Hamiltonian, one gets the free-energy increase per unit length of domain wall. It is given by[12,23]

$$f_d = \frac{2\sqrt{2}}{3}(-t)^{3/2}. \quad (10)$$

For the pure system, it is obvious that there exists no excited state with a closed domain wall. Since the free-energy increase is proportional to the length of the domain wall approximately, the solution with local minimum free energy must be that with zero length or infinite long straight domain wall. The infinite long straight domain wall causes an infinite free-energy increase, so they do not play important roles in phase transition.

However if the temperature field is not a constant, there exist saddle point solutions with closed domain walls. At first, let us see the simplest case, the SPE [Eq. (6)] with a round well

$$t(\mathbf{r}) = \begin{cases} t_w, & |\mathbf{r}| < 0.5 \\ t_b, & |\mathbf{r}| > 0.5. \end{cases} \quad (11)$$

The numerical results show that only if $t_w, t_b < 0$ and $t_w < t_b$, the excited-state solution with a domain wall can exist. This is the reason why we call the region $r < 0.5$ well. The region outside the well is called background. The situation with $t_w < 0, t_b > 0$ has been discussed for LOR.[21]

If $-t_w, -t_b \gg 1.0$, the saddle point solution is given by $\phi \approx \pm\sqrt{-t_b}$, $r > 0.5$; $\phi \approx \pm\sqrt{-t_w}$, $r < 0.5$. For the ground state the solution has the same sign all over the system. For the excited state, it has opposite sign inside and outside the well. Two typical excited-state solutions for $t_w = -1000$, $t_b = -600$ and $t_w = -1000$, $t_b = -880$ are shown in Fig. 1.

From these two solutions, one can see some qualitative properties of the excited-state solutions. The domain wall, where $\phi = 0$, is located outside the well. The radius of the domain wall for $t_b = -880$ is shorter than that for $t_b = -600$. That is to say, the radius decreases as the absolute value of t_b increases. In fact this is a general property.

From the numerical solution, it is found that only if $t_w \lesssim -4.0$ and $0 < t_b < t_{bc}$ the excited-state solution can exist. For a given t_w, the radius of the domain wall decreases as the t_b decreases. When t_b decreases to a threshold value t_{bc}, this excited-state solution disappears. The numerical result for t_{bc} is shown in Fig. 2.

The result that the excited-state solution disappears for $t_b < t_{bc}$ can be understood qualitatively from the rule of minimizing free energy. Consider the domain wall around the well. The domain-wall free energy depends on two quantities: its length (or radius) and the free-energy increase per unit length. The free-energy increase is contributed mainly

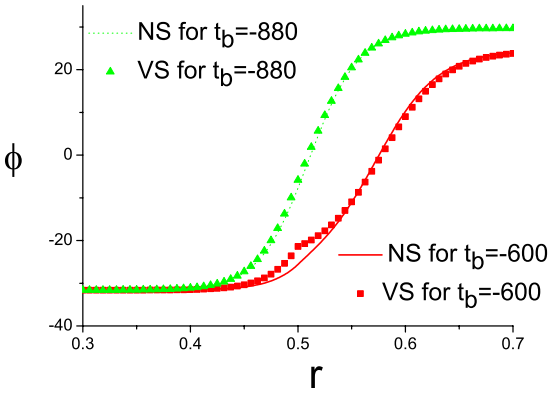

FIG. 1. (Color online) The excited-state solution for the round well with $t_w=-1000$, $t_b=-600$ and $t_w=-1000$, $t_b=-880$. "NS" and "VS"mean numerical solution and variational solution, respectively.

from region near the domain wall, where the absolute value of excited-state solution is remarkably smaller than the ground-state solution. Therefore we can imagine the domain wall a "wall with thickness." If the domain wall is located inside the well completely, the free energy per unit length is proportional to $(-t_w)^{3/2}$ [see Eq. (10)] approximately. If it is located outside the well completely, the free energy per unit length is proportional to $(-t_b)^{3/2}$ approximately. However in fact the domain wall is located partly inside the well and partly outside the well (see Fig. 1). There are two factors which determine the radius of domain wall. One is the difference $(-t_w)^{3/2}-(-t_b)^{3/2}$ and another is $(-t_b)^{3/2}$. The larger $(-t_w)^{3/2}-(-t_b)^{3/2}$ is, the less part of domain wall locates inside the well, hence the larger the radius is. The larger $(-t_b)^{3/2}$ is, the smaller the radius is.

For $|t_b| \ll |t_w|$, the domain wall is located mostly outside the well since increasing the part of domain wall inside the well will cause significant increase in free energy. As $|t_b|$ increases, the radius of domain wall will decrease to reduce the length of domain wall. Then the part of domain wall inside the well increases. For $t_b < t_{bc}$, the difference $(-t_w)^{3/2}-(-t_b)^{3/2}$ cannot resist the shrinking of the domain wall. Then the excited state disappears.

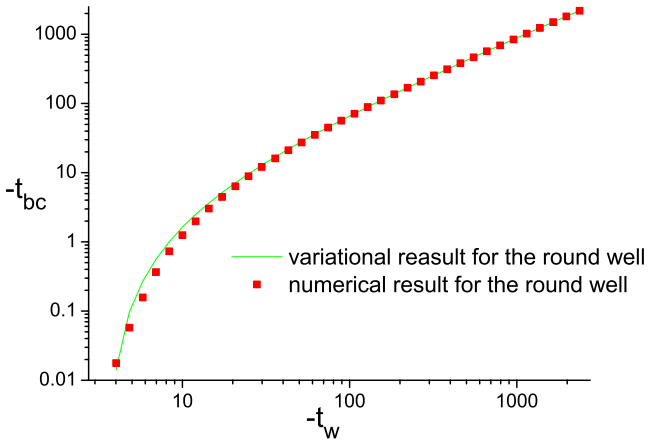

FIG. 2. (Color online) The numerical and variational results of t_{bc}. The green solid line is drawn from the variational solution of Eq. (22).

We may imagine the domain wall as a thread with tension [proportional to $(-t_b)^{3/2}$] and the well as a balloon with strength [proportional to $(-t_w)^{3/2}-(-t_b)^{3/2}$]. As t decreases, the tension increases, the thread (domain wall) shrinks. As the tension is larger than a threshold value, the balloon is torn.

For the excited-state solution, a variational solution is available. We choose the following trial solution:

$$\phi_1(\mathbf{r}) = \sqrt{-t_w}\,\tanh[\mu_1(r-r_1)]; r < 0.5,$$

$$\phi_2(\mathbf{r}) = \sqrt{-t_b}\,\tanh[\mu_2(r-r_2)]; r > 0.5, \tag{12}$$

where

$$\mu_1 = \sqrt{-t_w/2}; \quad \mu_2 = \sqrt{-t_b/2}. \tag{13}$$

At the well boundary $r=0.5$, it is required that the solution is continuous,

$$\sqrt{-t_w}\,\tanh[\mu_1(0.5-r_1)] = \sqrt{-t_b}\,\tanh[\mu_2(0.5-r_2)] \equiv \phi_d. \tag{14}$$

Thus the trial solution has a variational parameter ϕ_d.

The free energy of the trial solution is given by

$$\frac{F}{2\pi} = \int_0^{0.5}\left[\frac{1}{2}\left(\frac{d\phi_1}{dr}\right)^2 + \frac{1}{2}t_w\phi_1^2 + \frac{1}{4}\phi_1^4 + \frac{t_w^2}{4}\right]rdr + \int_{0.5}^{\infty}\left[\frac{1}{2}\left(\frac{d\phi_2}{dr}\right)^2 + \frac{1}{2}t_b\phi_2^2 + \frac{1}{4}\phi_2^4 + \frac{t_b^2}{4}\right]rdr. \tag{15}$$

We add a constant term to cancel the divergence and to be convenient for calculation. Here we cannot apply the formula (3) since the trial solution does not satisfy the SPE exactly.

Through some calculation, we get

$$\frac{1}{2\pi}\frac{dF}{d\phi_d} = \frac{\sqrt{-t_w}\left(\frac{2}{3}+\phi_0-\frac{1}{3}\phi_0^3\right)}{1+\phi_d/t_w} + \frac{\sqrt{2}}{4}(t_w-t_b) - \frac{2}{3}\left[\frac{t_w}{\sqrt{-t_w}-\phi_d} + \frac{t_b}{\sqrt{-t_b}+\phi_d}\right], \tag{16}$$

where

$$\phi_0 = \tanh(-\mu_1 r_1). \tag{17}$$

We adopt the approximation

$$\phi_0 = \tanh(-\mu_1 r_1) \approx -1, \tag{18}$$

because of $\mu_1 \gg 1$ and $r_1 \sim 0.5$.

Letting $dF/d\phi_d=0$ leads to

$$\phi_d^2 - a\phi_d - ab = 0, \tag{19}$$

where

$$a = \sqrt{-t_w} - \sqrt{-t_b} - \frac{4\sqrt{2}}{3},$$

$$b = \frac{\sqrt{t_w t_b}}{\sqrt{-t_w} - \sqrt{-t_b}}. \tag{20}$$

Solving it we get

$$\phi_d^{\pm} = \frac{1}{2}(a \pm \sqrt{a^2 + 4ab}). \tag{21}$$

Obviously it must have has $a > 0$ for a real solution. Therefore for a given t_w only if,

$$0 > t_b > t_{bc} = -\left(\sqrt{-t_w} - \frac{4\sqrt{2}}{3}\right)^2, \tag{22}$$

the domain wall exists. This equation gives the threshold value of the background temperature. The solid line in Fig. 2 is drawn according to this equation. As one can see the variational result agrees with the numerical result excellently.

The second derivative of the free energy with respect to ϕ_d is given by

$$\frac{1}{2\pi}\frac{d^2F}{d\phi_d^2} = \frac{2}{3}\left[\frac{1}{(1 - \phi_d/\sqrt{-t_w})^2} - \frac{1}{(1 + \phi_d/\sqrt{-t_b})^2}\right]. \tag{23}$$

Since $\phi_d^+ > 0$ and $\phi_d^- < 0$, one can see that $\phi_d = \phi_d^+$ is a solution with local maximum free energy and $\phi_d = \phi_d^-$ is the solution with local minimum free energy. Substituting

$$\phi_d = \phi_d^-, \tag{24}$$

into Eq. (12), we get the variational solution. The variational solutions $t_w = -1000$, $t_b = -600$ and $t_w = -1000$, $t_b = -880$ shown in Fig. 1 are obtained in this way.

If $|t_w - t_{bc}|/|t_w| \ll 1$ the threshold Eq. (22) is approximately given by

$$\frac{|t_w - t_{bc}|}{\sqrt{-t_w}} \approx \frac{8\sqrt{2}}{3}. \tag{25}$$

If the radius of the well is R rather than 0.5, one can get

$$\frac{|t_w - t_{bc}|}{\sqrt{-t_w}} \approx \frac{4\sqrt{2}}{3R}, \tag{26}$$

where transformations (5) is used. This formula is useful in the following discussion.

From this simple model, we draw two conclusions: (1) The domain wall may exist around a well, where the temperature is lower than out side. (2) For certain temperature in the well, there is a threshold value for the background, above which the domain wall can exist. The threshold value is approximately given by Eq. (22).

IV. DOMAIN WALL ON A WELL LATTICE

As a warm-up, we shall solve the SPE on a well lattice defined by

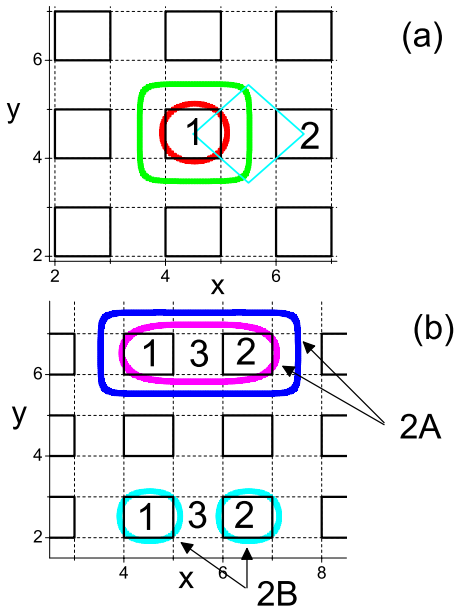

FIG. 3. (Color online) (a) The domain wall around one well. (b) The domain walls around two wells.

$$t(\mathbf{r}) = \begin{cases} & 2m < x < 2m+1 \\ t - t_{bw}, & \\ & 2n < y < 2n+1 \\ t, & \text{other regions}, \end{cases} \tag{27}$$

where $m, n = 0, \pm 1, \pm 2, \ldots$. We consider $t_{bw} > 0$. The regions with temperature $t - t_{bw}$ and t are called wells and background, respectively. The square wells, whose sizes are 1×1, are shown schematically in Fig. 3 with black solid line. The background is also divided into blocks of size 1×1, which are drawn in dashed lines. A cell is composed of one well and three background blocks. Its size is 2×2. A spin model with such a temperature field is given in Appendix A.

In this section we take

$$t_{bw} = 40.0. \tag{28}$$

There is no special significance of this temperature because the results are qualitatively the same only if $t_{bw} \gtrsim 10$. In addition we study the excited states on this well lattice only to get some insights, which may help us to understand the excited states on the lattice with random temperature.

The numerical method is similar to that in the previous work[20] and can be found in Ref. 24. Dividing the lattice into a uniform two-dimensional grid and replacing derivative expressions with approximately equivalent difference quotients, the SPE is solved recursively. The step of grid is denoted by h. In this section it has $h = 0.05$. The precision of the solution is $\Sigma_{ij}(\phi_{i,j}^{(n+1)} - \phi_{i,j}^{(n)})^2 / \Sigma_{ij}(\phi_{i,j}^{(n+1)})^2 < 10^{-14}$, where $\phi_{i,j}^{(n)}$ is the solution of nth iteration.

The numerical result shows that as $t < 28.9 \pm 0.1$ and $t - t_{bw} < -11.1 \pm 0.1$ the saddle point solution can be nonzero. If the initial values on the lattice are positive (or negative) all over the lattice, one get the ground-state solution with no

domain wall. If the signs of initial values are taken randomly, one will get the excited-state solutions.

The ground-state solution can be referred to Ref. 20. For $0<t<28.9\pm0.1$ it is periodic and nonzero in wells and decays to zero quickly outside the wells. For $-t\ll1$, the solution is approximately $\sqrt{-(t-t_{bw})}$ in wells and $\sqrt{-t}$ outside the wells.

A. Small size domain walls

The simplest excited-state solution is that the order parameter in one well is opposite to that in other wells. Then a domain wall exists around the well (marked by "1") as shown in Fig. 3(a). The outer (in green) and inner (in red) curves are the domain walls at temperature $t=28.9$, -80.0, respectively. For $28.9\pm0.1>t>-85.77\pm0.01$ this excited-state solution exists. At temperature $t=28.9$, the domain wall is almost a square, and lies almost at the boundary of cell. As t decreases, the length of domain wall becomes shorter and shorter and the domain wall becomes rounder and rounder. At t below -85.77 ± 0.01 this state no longer exists. The disappearance of this state can be well explained by the discussion in the above section [see Eq. (25)]. The square formed by four diagonal lines in cyan starting from the centers of 1 and 2 is not relevant to the present discussion and useful in Sec. IV B.

This excited state is obtained numerically as follows. At first the initial value of $\phi^{(0)}$ is assigned to be $-\sqrt{-(t-t_{bw})}$ in well 1 and $\sqrt{-(t-t_{bw})}$ in other wells, and zero outside wells. Then we solve the SPE iteratively.

Two other simple excited states are those with a domain wall around two nearest neighbored wells, as shown in Fig. 3(b). The upper part and the lower part represent two different excited states. We denote the upper part and the lower part state 2A and 2B, respectively. For $-105.24\pm0.1<t<28.9\pm0.1$ state 2A exists. The outer (in blue) and inner (in magenta) curves in the upper part of Fig. 3(a) are the domain wall 2A at temperature $t=28.9$, -105.0, respectively. For $-46.9\pm0.1>t>-85.7\pm0.1$ state 2B exists. The curve (in cyan) in the lower part of Fig. 3(b) is the domain wall 2B at temperature $t=-80.0$. The difference between states 2A and 2B lies at the region (marked by "3") between the two wells (marked by "1" and "2"). In state 2A, the sign at "3" is the same as that at "1" and "2," while in state 2B is opposite.

TABLE I. The temperature ranges of existence of domain walls shown in Fig. 4.

Domain wall	Temperature range of existence
a	$-105.05\pm0.05<t<-12.725\pm0.025$
b	$-118.9\pm0.1<t<28.9\pm0.1$
c	$-182.4\pm0.1<t<28.9\pm0.1$
d	$-137.8\pm0.1<t<28.9\pm0.1$
e	$-256.75\pm0.25<t<28.9\pm0.1$
f	$-85.85\pm0.05<t<-47.85\pm0.05$
g	$-85.92\pm0.01<t<-63.95\pm0.05$

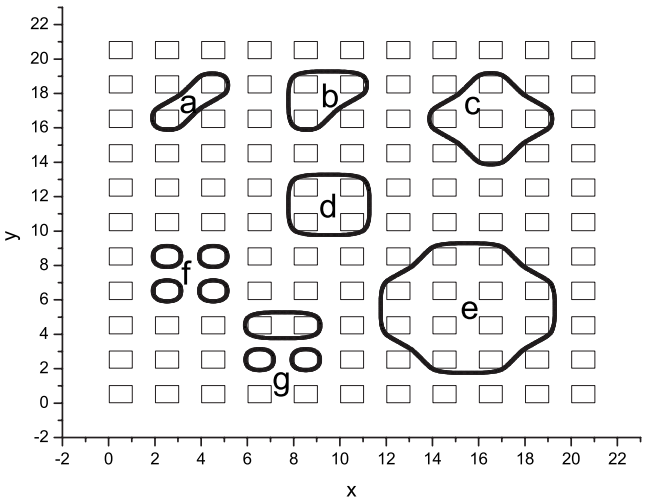

FIG. 4. Some domain walls with simple structure.

More domain walls with simple structure at $t=-80.0$ are shown in Fig. 4 and their temperature ranges of existence are given in Table I. It can be seen that the larger the radius of curvature is, the lower the disappearing temperature is. This is consistent to the criterion [Eq. (26)] of disappearing of a domain wall.

B. Adiabatic evolution of an excited state

In the above subsection we show the evolution of some simple excited states. How about an arbitrary excited state? We show the evolution of a typical excited state in Fig. 5. The colored curves are domain walls. The system size in our numerical solution is 100×100 and we show its part of $20<x,y<40$.

At first, we solve an excited-state solution of $t=20$. The initial value of ϕ is assigned to be $\sigma_i\Phi_i$ in each well and to be zero outside wells. Here $\sigma_i=\pm1$ is taken randomly. Φ_i can be different arbitrary positive numbers in different wells. It is found that only if the iteration is convergent the solution depends only on the initial signs $\{\sigma_i\}$ in each well, but the initial amplitude of Φ_i, which only influence the converging

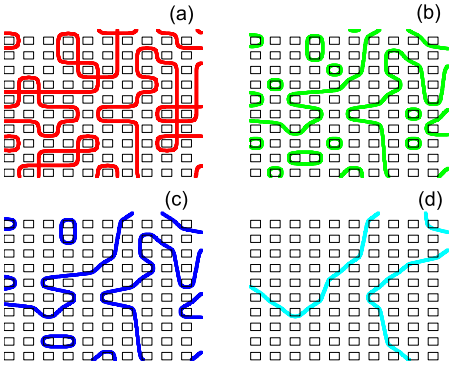

FIG. 5. (Color online) The evolution of an excited state. The colored curves are the domain walls and the thin square are the boundary of the wells. (a) $t=0$. (b) $t=-60$. (c) $t=-100$. (d) $t=-160$.

rate of the iteration. In order to make the iteration converging faster we usually take that $\Phi_i=\sqrt{-(t-t_{bw})}$ in calculation.

Then we solve the excited-state solution of $t=10$ taking the solution of $t=20$ as the initial value. Then we solve the excited-state solution of $t=0$ taking the solution of $t=10$ as the initial value, and so on. We call this process the "adiabatic evolution" (AE) of an excited-state solution.

At temperature $t=0$, as one can see in Fig. 5(a), the domain wall are located almost on the boundary of cells. The corners are sharp. In addition, it seems that there are intersecting points in the domain wall in Fig. 5(a). In fact they are composed of separated corners if they were inspected carefully. In Fig. 5(b), where the temperature is $t=-60$, these corners are separated farther. Compared with Fig. 5(a), the domain wall in Fig. 5(b) becomes rounder, bent, and shorter.

At $t=-100$ as shown in Fig. 5(c), the domain walls around single well disappear. At $t=-160$ as shown in Fig. 5(d), the domain walls around two nearest-neighbored wells disappear. The corners with small radius of curvature in Fig. 5(c) also disappear in Fig. 5(d). The domain wall becomes smoother.

As shown in Fig. 4 and Table I, for $t<-118.9\pm0.1$, domain wall "2A" disappears; for $t<-137.8\pm0.1$, domain wall "d" disappears, etc. The disappearance of the closed domain wall and the corners with small radius of curvature can be explained by Eq. (26). This can be shown by letting $t_w=t-t_{bw}$; $t_b=t$ and assuming that the round well results are valid approximately for the square well. As t decreases, only the domain walls with enough large radius of curvature can survive. Therefore as temperature t decreases, the domain wall becomes shorter and shorter, smoother and smoother.

The disappearing of closed domain wall with small size and the corners with small radius of curvature means that a lot states evolve to one state. It is easily imagined that if some closed domain walls around single well, as shown in Fig. 5(b), are removed, one will get different excited states. However these different states will evolve to the same state, as shown in Fig. 5(c), as t decreases below -85.7 ± 0.1 because then all the domain walls around single well will disappear.

C. Domain wall's length and its free energy per unit length

To describe an excited state, we calculate the total length of all domain walls, which is defined by $\phi_i(\mathbf{r})=0$. It is denoted by

$$\Lambda = \text{length of domain wall.} \tag{29}$$

Then we define the length of domain wall per unit area by

$$\zeta = \frac{\Lambda}{S}, \tag{30}$$

where S is the area of the system.

For an excited-state solution, we also calculate the autocorrelation function and the correlation length defined in.[21] We denote the correlation length for the excited states ξ_e. We show the results of $\zeta, \xi_e, 1/(\zeta\xi_e)$ in Fig. 6, where each data is average of 32 solutions on the lattice with size 100×100.

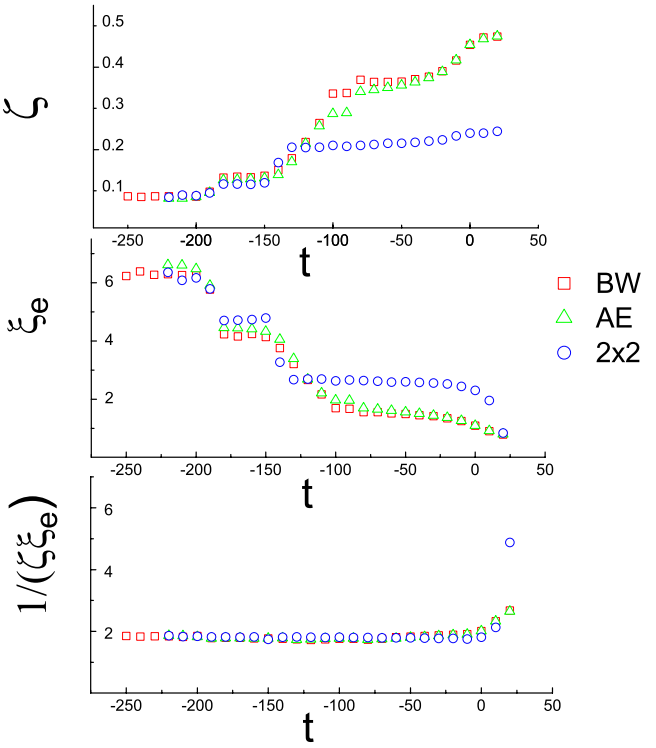

FIG. 6. (Color online) The domain-wall length per unit area and the correlation length at different temperatures.

The results of adiabatic evolved solutions are labeled by AE in Figs. 6 and 7.

The length of domain wall decreases as the temperature decreases. The curve seems to be composed of some steps. The jumps of ζ correspond to the disappearance of certain domain walls. For example, there is a jump of ζ as t decreases from -80 to -90 because the domain walls around single well disappear at temperature $t=-85.7\pm0.1$ as mentioned above. If more data for $-90<t<-80$ are shown, this jump can seen clearly at $t\approx-85.7$.

The correlation length ξ_e is also shown in Fig. 6. In fact, one can see the significance of ξ_e from the data. For $t>0$, the correlation length ξ_e is less than 1, for example, $\xi_e\approx0.8$ at $t=20$. For $-t\gg1$, at wells the solution is $|\phi_e|\approx\sqrt{-(t-t_w)}$ and decays to exponentially small in the scale $1/\sqrt{t}$ at background. The signs at wells are the same as the initial ones,

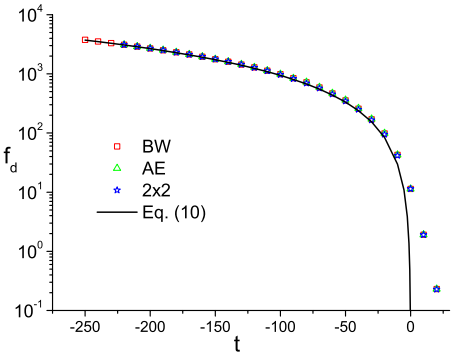

FIG. 7. (Color online) The free energy per unit length of domain-wall length at different temperatures.

which are random and not correlated. Therefore the correlation length ξ_e is approximately the size of wells.

The correlation length ξ_e increases as t decreases. For $t<-t_w=-40$, the correlation length is larger than the well size. For example it is $\xi_e=1.69$ at $t=-100$. It equals approximately twice size of wells. At this temperature the domain walls around single well disappear and the smallest closed domain wall must surround two wells. For $-180<t<-150$, the correlation length is about 4. At this temperature range, the smallest domain wall is "c" which is shown in Fig. 4, and its size is approximately 4×4. Therefore the correlation length is approximately the size of the smallest closed domain wall.

The free energy of the solution is calculated according to

$$F_{g,e}=-\frac{1}{4}\int dxdy\phi_{g,e}^4, \tag{31}$$

where the subscripts g,e represent ground state and excited states, respectively. This equation is obtained from Eq. (3) with $g=1$. For each excited-state solution, we calculate the average free energy per unit length of domain wall,

$$f_d=(F_e-F_g)/\Lambda. \tag{32}$$

The dependence of f_d on the temperature is shown in Fig. 7, where each data is average of 32 solutions on the lattice with size 100×100. For $t>0$, f_d is small but not zero because of the nonzero solution at wells and their extension to the background. For $t<-t_{bw}=-40$, it approaches the result for the straight domain wall in pure systems, i.e., Eq. (10). Then the domain wall is located almost at background. If every segment of the domain wall is regarded as the straight domain wall in pure systems with temperature t, the free energy per unit length is just given by Eq. (10). In fact f_d is a bit larger than the result in Eq. (10) because of the curvature of domain wall and the influence of well.

However there are some excited states missed in the above way. For example, the excited state 2B cannot be obtained using AE method. For $t<0$, the excited solution depends on not only the initial signs of wells but also those of background blocks. The excited state 2B is obtained with the initial signs at blocks 1, 2 the same and opposite to that at block 3 and other blocks. This kind of initial value is called "BW" since both the wells and the background are concerned.

For an arbitrary solution with BW initial value, the initial value of ϕ is assigned to be $\sigma_i\Phi_i$ in every 1×1 block as shown in Fig. 3, including well and background. Here $\sigma_i=\pm1$ is taken randomly. It is taken that $\Phi_i=\sqrt{-(t-t_{bw})}$ for a well; $\Phi_i=\sqrt{-t}$ if $t<0$ for a background block. Obviously the BW solutions are more than "AE" solutions and include all the AE solutions.

As shown in Fig. 6, the results of BW and AE have some differences, but the differences are relatively small. For $-100<t<-60$ the domain-wall length ζ of BW is obviously larger than that of AE because of the domain walls "a,f,g" in Fig. 4, which are absent in AE solutions. For $t<-100$, their difference is small.

In Appendix B, we argue that the exceeding BW excited states compared with AE states are not many as it seems to be. Therefore we can ignore the exceeding BW states in discussing the phase transition approximately.

D. Block model and mapping to an Ising model

For $-85.7\pm0.1<t<28.9\pm0.1$, it is found that the signs at the center of wells do not change in the iteration for the AE solutions. This can be simply verified in the numerical calculation by comparing the initial signs and the final signs in the iteration. That means a set of initial signs $\{\sigma_i\}$ at the wells corresponds to an excited state. The configurations of the excited states are the same as those for Ising model.

At about $t<-85.7$, the domain wall around single well disappears and at about $t<-105$, the domain walls around two wells, "2A" shown in Fig. 3(b) and "a" in Fig. 4, disappear. In convenience, we call the wells surrounded by a closed domain wall a "cluster." Obviously, at about $-105<t<-85.7$, the smallest cluster has two wells. Larger size clusters are allowable, such as "b,c,e,d" in Fig. 4. However some large size clusters can be decomposed into small size clusters. For example, the cluster "e" in Fig. 4 can be decomposed into two clusters of "2A" in Fig. 3(b). The cluster "2A" shown in Fig. 3(b) and "a, b" in Fig. 4 are elementary and irreducible. Of course there are many other irreducible clusters. It should be noted that one well cluster is not allowable and is not an elementary cluster.

The above picture can be simplified further, if the phase transition takes place in $-105<t<-85.7$. The phase transition here is referred to the appearance of long-range order due the coupling between the clusters. As we known, near the critical point the large scale fluctuation is most important. That is to say, configurations with large size clusters are important. Large size clusters can be approximately decomposed into the cluster "2A" shown in Fig. 3(b) since the edge can be ignored if the cluster is large enough. Therefore two horizontal wells as surrounded by domain wall "2A" in Fig. 3(b) is only one concerned elementary cluster at temperatures $-105<t<-85.7$.

At about $t<105$, the domain walls around two wells, "2A" shown in Fig. 3(b) and "a" in Fig. 4, disappear. At about $t<119$, the domain wall around three wells, "b" in Fig. 4, disappears. At about $-119<t<-105$, the clusters, "b, e" in Fig. 4, are irreducible. Larger size clusters are allowable, such as "d" in Fig. 4. In addition, there is a requirement for the allowable clusters. The radius of curvature on the domain wall around the cluster must be larger than the minimum on the domain wall, "b" in Fig. 4. Therefore most large size clusters can be approximately decomposed into the cluster, "b" in Fig. 4. Similarly if the phase transition takes place in $-119<t<-105$, the cluster, "b" in Fig. 4, is the concerned elementary cluster.

Similar discussion can be continued for lower temperatures. Although the situation at about $t<-85.7$ is more complicated than that at about $t>-85.7$, the picture is qualitatively the same.

According to the above discussion we can propose a unified block model to describe the domain wall and phase tran-

sition approximately at all temperatures. Suppose the system is divided into $n=S/(b\times b)$ square blocks with size $b\times b$. The block is referred to the elementary cluster mentioned above. For $t>-85.7$ the block has one well. For $-105<t<-85.7$, the block has two adjoining wells. For $-119<t<-105$, the block has three wells, as domain wall "b" shown in Fig. 4. Although these elementary blocks have irregular shapes, we deal them as square for simplicity.

The domain wells exist only between these blocks and cannot cross these blocks. Because the initial value is random, in the solutions the signs at blocks are random. Generally half blocks have positive sign and half blocks have negative sign. Accordingly half couples of adjoining blocks have opposite signs. There are $2n$ couples of adjoining blocks, so there are n couples of adjoining blocks having opposite signs. Moreover suppose the length of domain wall between two adjoining blocks is the size of blocks b; hence, the total length of domain wall is nb. On the other hand, as we know, the total length of domain wall is ζS. Therefore we have

$$b = 1/\zeta. \tag{33}$$

As temperature decreases block (the elementary cluster) becomes larger and larger, so the domain-wall length becomes shorter and shorter. This explanation agrees with the above discussion.

In order to test the above model further, we have carried out numerical solution with anther kind of initial value. It is labeled by "2×2" in Fig. 6 and 7. For "2×2" initial value, the lattice is divided into blocks, each of which contains 2×2 wells. The random signs are assigned to blocks rather than single wells. As shown Fig. 6, the results for AE, BW, and "2×2" differ much for $t>-120$ and little for $t<-120$. In AE, BW solutions, there are the domain walls surrounding 1, 2, or 3 wells, while in "2×2" solutions there is no such domain wall. It is natural that their results are different for $t>-120$. For $t<120$, in AE, BW solutions, the domain walls surrounding 1, 2, or 3 wells disappear, and the smallest domain wall surrounds 2×2 wells. This constraint on the domain-wall size is the same as in "2×2" solutions. Therefore their results are approximately the same. In other words, the AE, BW solutions can be described by the above block model with block size 2×2 for $t<-120$.

For $t<-t_w=-40$ it has $1/(\zeta\xi_e)\approx 1.8$ as shown in Fig. 6. This leads to $b\approx 1.8\xi_e$. Thus the correlation length ξ_e has a well-defined significance in the block model: the block size is about twice of ξ_e.

Now we discuss the phase transition on the well lattice. For $-85.7\pm 0.1<t<28.9\pm 0.1$, the configurations of the excited states are the same as those for Ising model. In this temperature range, the partition function at the level of saddle point solution can be mapped to an Ising model approximately.

Consider two adjoining wells, say wells 1 and 2 in Fig. 3(a). If they have the same signs, there is no domain wall between them. Otherwise there is a segment of domain wall between them. Assuming the free-energy increase due to this segment is $K_{1,2}$, which may be defined as

$$K_{1,2} = g^{-1}l^{-2}\int_{12} dxdy\left[\frac{1}{4}\phi_g^4 - \frac{1}{4}\phi_e^4\right], \tag{34}$$

where the integration is carried out in the region surrounded by the four diagonal cyan lines starting from the centers of 1 and 2. The original parameters g,l given in Appendix A are considered and the transformation Eq. (8) is used. Then for two adjoining wells, if there is a segment of domain wall between them, the free-energy increase due to these two wells is given by $-K_{ij}(\sigma_i\sigma_j-1)/2$.

Obviously the coupling $K_{i,j}$ defined as Eq. (34) is valid approximately. Since as shown in Fig. 5, the domain-wall length between two adjoining wells defined in Eq. (34) depends on the signs at next-nearest-neighbored wells and next-next, etc. Therefore a more accurate effective Hamiltonian should include the coupling with distant wells and four wells' coupling, six well's coupling, etc. In principle the couplings can be obtained from the numerical calculations of free energies of many excited states.

However the nearest neighbors' coupling is most important. Therefore in the lowest approximation the free-energy increase in the whole lattice can be given by

$$F_e - F_g \approx -\sum_{i,j}\frac{K_{ij}}{2}(\sigma_i\sigma_j - 1), \tag{35}$$

where the summation is over nearest neighbors. The partition function Eq. (4) becomes

$$Z \approx e^{-F_g-\Sigma_{\langle i,j\rangle}K_{ij}/2}\sum_{\{\sigma_i\}}\exp\left\{\sum_{\langle i,j\rangle}\frac{K_{ij}}{2}\sigma_i\sigma_j\right\}. \tag{36}$$

Obviously this is an Ising model with coupling constants $K_{ij}/2$ for nearest neighbors. If more accurate result is needed, the couplings with distant wells and four wells' coupling, six wells' coupling, etc, can be introduced.

Similarly for $t<85.7$, the partition function at the level of saddle point solution can also be mapped to an Ising model approximately. However the block size increases as temperature decreases. The coupling between two adjoining blocks can also be defined as mentioned above. As the temperature decreases, the couplings increase. The average coupling between two adjoining blocks can be estimated with

$$K_{i,j} \sim g^{-1}l^{-2}bf_d = g^{-1}l^{-2}f_d/\zeta, \tag{37}$$

because the length of segment of domain wall between two adjoining blocks is approximately equal to the block size b.

As the couplings increase to be critical, phase transition will take place. Because this system has the lattice translational invariance, the effective Hamiltonian at the level of saddle point solution has also the lattice translational invariance. Hence the universality of phase transition should belong to the same universality of the usual Ising model. However there is an intermediate characterizing scale beside the correlation length of critical fluctuation. That is the correlation length of the excited solution ξ_e, which is the size of blocks.

From well lattice model, we get

(1) The result of domain-wall length can be described by a block model [see Eq. (33)].

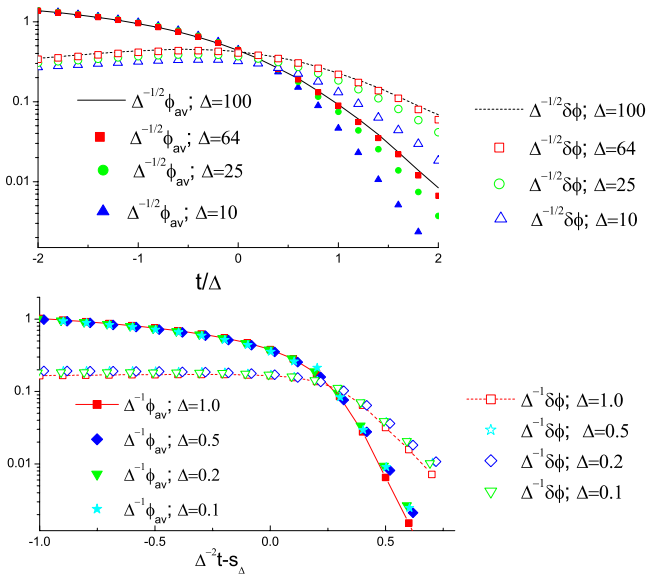

FIG. 8. (Color online) The average and fluctuation of the ground-state solutions.

(2) The partition function at the level of saddle point solution is approximately equal to an Ising model like Eq. (36), in which the block behaves like a superspin.

V. EXCITED STATES ON A LATTICE WITH RANDOM TEMPERATURE

We have carried out intensive numerical calculation on the lattice with random temperature with $0.1<\Delta<100$ and $g=l=1$ for Eq. (6). For $\Delta=100$, 64, 25, 10, the lattice size and the step are $L=100$, $h=0.05$, respectively. For $\Delta\leq 1.0$, we take $L/h=2000$ and $h=0.2$, 0.25, 0.2, 0.1 for $\Delta=1.0$, 0.5, 0.2, 0.1, respectively.

Given a realization of $\tilde{t}$ on a finite-size lattice, there are two ground states and many excited states. If the initial values have the same signs, one will get the ground-state solution, denoted by ϕ_g. If the signs of initial value at cells are randomly given, one can get an excited-state solution, denoted by ϕ_e. A sample is referred to a solution with certain realization of random temperature and certain initial values. Each data in Figs. 8–12 is the average over 32 samples. The deviations around the average for most data are less than 5%.

A. Distribution functions in inhomogeneous and inhomogeneous regime

The ground state had been studied in the previous work.[21] The average ϕ_{av} and fluctuation δ_ϕ for the ground-state solutions are shown in Fig. 8. The temperature range in the figure is wider than that in the previous work and the forms of figures are also different. I show this figure because it is necessary in the discussion.

As shown in Fig. 8, for the strongly disordered case, i.e., $\Delta>1$, it has that $\phi_{av}/\sqrt{\Delta}$ vs t/Δ are approximately equal for different Δ. The curves for $\Delta=100$, 64, 25 indeed coincide approximately. It also has $\delta_\phi/\sqrt{\Delta}$ vs t/Δ are approximately

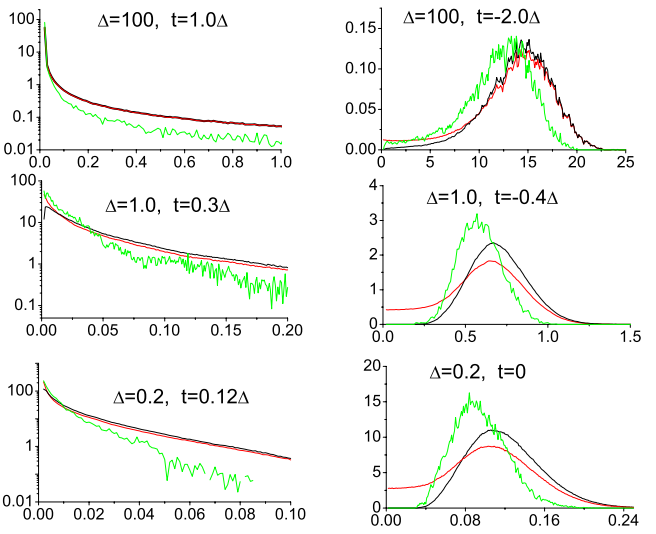

FIG. 9. (Color online) The distributions ρ_g (black), ρ_e (red), and ρ_d (green) of the absolute value of ϕ.

equal for different Δ. However the coincidence for $\delta_\phi/\sqrt{\Delta}$ vs t/Δ is not good as $\phi_{av}/\sqrt{\Delta}$ vs t/Δ.

For the weakly disordered cases, $\Delta\leq 1$, the scaling relations for ϕ_{av} is given by $\phi_{av}(\Delta,t,1)\approx\Delta\phi_{av}(1,\Delta^{-2}t-s_\Delta,1)$, where s_Δ is a temperature shift.[20] In Fig. 8, it has $s_\Delta=0.1077$, 0.2815, 0.4888 for $\Delta=0.5$, 0.2, 0.1, respectively. For δ_ϕ, it has a similar scaling relation.

As one can see in Fig. 8 at the high-temperature side the average ϕ_{av} is much smaller than the fluctuation δ_ϕ and at the low-temperature side the situation is contrary. This feature indicates that at the high temperature the solution is very inhomogeneous and at the low temperature the solution is homogeneous. On one hand, for $t\gg\Delta$ there are rare LOR, in which the saddle point is nonzero, and in other regions it is nearly zero. It is easy to show that in this case it should have

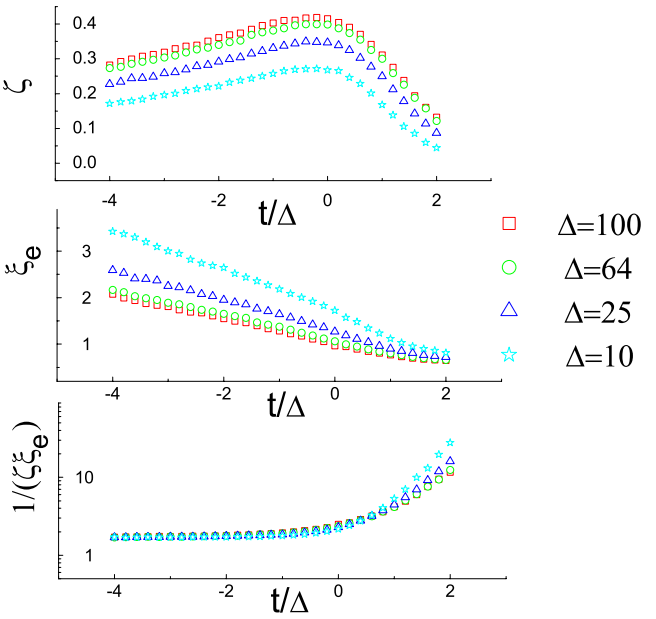

FIG. 10. (Color online) The domain-wall length and the correlation length of excited-state solutions for strongly disordered cases.

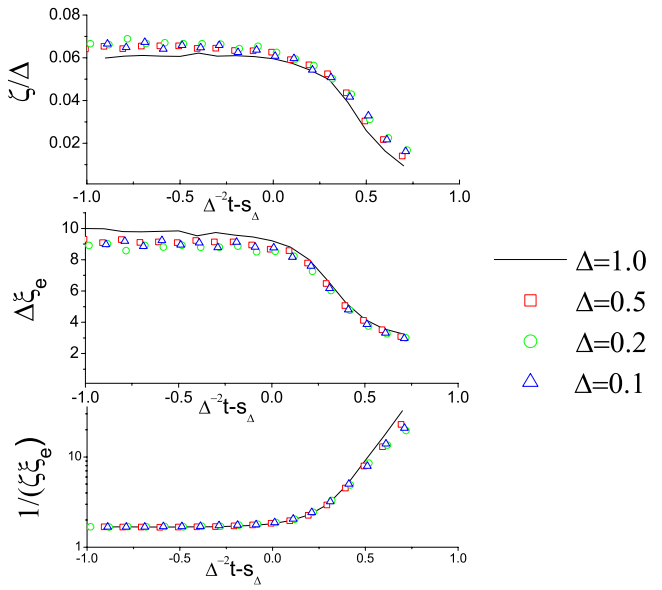

FIG. 11. (Color online) The domain-wall length and the correlation length of excited-state solutions for weakly disordered cases.

$\delta_\phi/\phi_{av} \gg 1$, although the absolute value of δ_ϕ is very small. On the other hand, for $-t \gg \Delta$ the random part $\tilde{t}_i$ is only a perturbation, the fluctuation δ_ϕ is much smaller than the average. The solution should be approximately uniform. Then it has $\delta_\phi/\phi_{av} \ll 1$. Therefore we can adopt a simple criterion: if $\delta_\phi/\phi_{av} > 1$ the solution is inhomogeneous and if $\delta_\phi/\phi_{av} < 1$ the solution is homogeneous.

Given a realization of temperature $t+\tilde{t}_i$, one can get two ground-state solutions (with positive or negative sign) and many excited-state solution. If the absolute values of ground and excited solutions for the same realization of temperature $t+\tilde{t}_i$ are compared, they differ mainly nearby the domain wall, where the free-energy increase stems from.

To see the difference and relation between the ground-state and excited-state solutions, we may introduce three distribution functions: ρ_g, ρ_e, and ρ_d. For the ground-state solution ϕ_g is defined by

$$\rho_g(z) = \frac{dS_{gz}}{Sdz}, \tag{38}$$

where dS_{gz} is the total area of the regions where $z < \phi_g < z + dz$. For the excited-state solution, ϕ_e is defined by

$$\rho_e(z) = \frac{dS_{ez}}{Sdz}, \tag{39}$$

where dS_{ez} is the total area of the regions where $z < |\phi_e| < z + dz$.

The third distribution function ρ_d is defined for both the excited- and ground-state solutions. From Eq. (31) it is seen that the free-energy increases is mainly contributed from the region near the domain wall. Further more the free-energy increase is determined by the ground-state solution at the region near the domain wall. So we define

$$\rho_d(z) = \frac{dL_{gz}}{\Lambda dz}, \tag{40}$$

where Λ is the total length of domain wall and dL_{gz} is the total length of the domain wall, where $z < \phi_d < z + dz$ and ϕ_d is the ground-state solution at the domain wall, where $\phi_e = 0$.

Typical distributions for $\Delta = 100$, $\Delta = 1.0$, $\Delta = 0.2$ are shown in Fig. 9. The three distribution functions ρ_g, ρ_e, and ρ_d are given in black, green, and red curves, respectively. There is a common feature in these distributions. The probability with large ϕ_d is smaller than those with the same ϕ_g and $|\phi_e|$ and accordingly the probability with small ϕ_d is larger. This is because the domain wall is located at regions with higher temperature.

The three distribution functions ρ_g, ρ_e, and ρ_d are approximately the same in all cases. So through the results for ground-state solutions shown in Fig. 8, we know the qualitative properties of excited-state solution, and the local free-energy increase due the domain wall.

Generally inhomogeneous regime is at the side of $t > 0$. In this regime, the absolute value of solution differs greatly. For $t > \Delta$, the cells with $t + \tilde{t}_i < 0$ are rare. Only at these cells, the solution is not zero, and at other cells the solution is exponentially small. Therefore the probability of ϕ_g with large value is exponentially small. The distribution is Poison type. Typical distributions in inhomogeneous regime for $\Delta = 100$, $t = 1.0\Delta$; $\Delta = 1.0$, $t = 0.3\Delta$; and $\Delta = 0.2$, $t = 0.12\Delta$ are shown in the three left subfigures in Fig. 9.

Homogeneous regime is at the side of $t < 0$. For $-t < \Delta$, the temperatures in most cells are negative and the random part can be regarded as a perturbation so the distribution is Maxwellian. Typical distributions for $\Delta = 100$, $t = -2.0\Delta$; $\Delta = 1.0$, $t = -0.4\Delta$; and $\Delta = 0.2$, $t = 0$ are shown in the three right subfigures in Fig. 9.

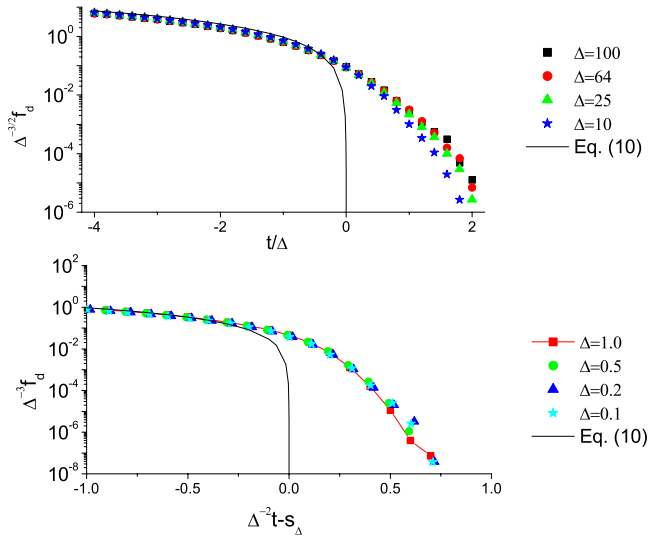

FIG. 12. (Color online) The free energy per unit length for strongly and weakly disordered cases.

B. Wells and background

The numerical results for the domain-wall length per unit area ζ and the correlation length ξ_e are shown in Figs. 10 and

11. The free energy per unit length of domain wall is shown in Fig. 12.

For the strongly disordered cases, $\Delta \gg 1$, the temperature is scaled with Δ as for the ground-state solutions.[21] For the excited states we expect the same scaling. Then the free-energy increase should be scaled with $\Delta^{3/2}$. This is why the temperature and free-energy increase are scaled with Δ and $\Delta^{3/2}$ in Figs. 10 and 12 for $\Delta \gg 1$.

For the weakly disordered cases, applying the coarse-grained approximation,[21] one can get

$$\zeta(\Delta,t,1) \approx \Delta\zeta(1,\Delta^{-2}t - s_\Delta,1), \tag{41}$$

for the domain-wall length per unit area ζ. The correlation length of excited states has a similar scaling relation. Through dimension analysis, one can get that the free energy per unit length of domain wall obeys

$$f_d(\Delta,t,1) \approx \Delta^3 f_d(1,\Delta^{-3}t - s_\Delta,1). \tag{42}$$

The data in Figs. 11 and 12 are scaled with the above scaling relations.

In well lattice model, there are two temperatures. So the lattice can be simply classified into two kinds of regions: well and background. The domain wall is located almost in background generally. On the random temperature lattice, the temperature is random. It seems that one cannot classify the lattices into two kinds of regions. However it is found that this classification still works well.

For the strongly disordered cases, $\Delta \gg 1$, the definitions of well and background is simple and clear. A cell is a well if its temperature is $t+\tilde{t}_i < 0$ and lower than its four adjoining cells. Otherwise it is background. Accordingly this definition, the probability that a cell is a well is given by

$$P_w\left(\frac{t}{\Delta}\right) = \left(\frac{1}{\sqrt{2\pi}}\right)^5 \int_{-\infty}^{-t/\Delta} e^{-y^2}\left[\int_y^{\infty} e^{-y'^2}dy'\right]^4 dy. \tag{43}$$

Obviously the probability of well is very small for $t \gg \Delta$ since the cells with negative temperature are rare. It increases as temperature decreases. It changes drastically in the range $2\Delta > t > 0$. It reaches 0.1937 at $t=0$.

For $-t/\Delta \gg 1$, it approaches its maximum 0.2. It can be easily shown that the integral for $t/\Delta \to \infty$ is 1/5. This limit value has a simple explanation. As $-t/\Delta \to \infty$, the probability is equivalent to that described as follows. Assign five random numbers in Gaussian distribution to five cells, a cell and its four nearest neighbors. The probability that the central cell has the minimum number among these five cells is 1/5.

Like the well lattice, the domain wall is located in the background and it surround the wells, which are defined above. As an example, we show four excited states for $\Delta = 100, t = 0.0$ on 10×10 lattice in Figs. 13(a)–13(c). The squares in black solid line are wells defined above. The colored curves are domain walls. The temperature realizations are the same in these three subfigures. The excited states in Figs. 13(a) and 13(b) are obtained with different initial values. In Fig. 13(c), the curves are the overlapping of four excited states, including the excited states shown in Figs. 13(a) and 13(b). As shown in Fig. 13(c), the domain wall is located in background and it surround the wells.

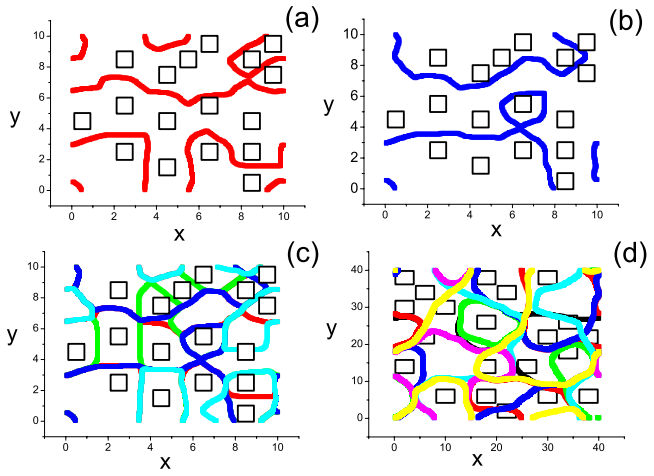

FIG. 13. (Color online) The wells and blocks on the lattice with random temperature.

As shown in Fig. 13(c), the overlapping of the domain walls of four excited-state solutions form curves which divide the system into blocks clearly. In fact these curves are the boundary of blocks because the domain wall is located on them for any arbitrary excited-state solution. We can verify this by the numerical solution in the following way. We choose an arbitrary well in Fig. 13(c), and let the sign of initial value in this well is opposite to that in other wells. Solving SPE with this initial value, we get the domain wall around this single well. It is found that this domain wall coincide the overlap of the four excited states shown in Fig. 13(c).

If so the blocks have different sizes and irregular shapes, and the well's positions are random. Although the block sizes are not uniform and the blocks are randomly located spatially, we expect that the excited solutions should be described by the block model defined for the well lattice model [see Eq. (33)].

Using the block model, the numerical results for $\Delta \gg 1$ in Figs. 10 and 11 can be well explained. At high temperatures $t > 0$, the wells are rare; hence the number of blocks is small so the domain walls are sparse. Then the domain-wall length per unit area ζ is small. As temperature decreases, the wells become more and more and the blocks become more and more, so the domain walls become denser and denser. Then ζ increases. The correlation length ξ_e is about 1. It reflects the size of LOR, which is localized in wells. The block size $b = 1/\zeta$ is the average distance between LOR, so it has $b \gg \xi_e$.

For $\Delta = 100$, the domain-wall length per unit area reaches its maximum (≈ 0.42) at $t=0$. Even this maximum can be explained by the block model. At $t=0$, about 1/5 of cells are cells [see Eq. (43)], so the average area of blocks is 5 assuming that every cell forms a block. The average size of block is $\sqrt{5}$. Accordingly the domain length per unit area should be $1/\sqrt{5} \approx 0.447$.

At $t=0$, the domain-wall length per unit area ζ decreases as Δ decreases, although the numbers of wells are equal for different Δ. In addition, ζ also decreases as temperature decreases for $\Delta = 100$ and $t < 0$, although the numbers of wells varies little. This is because that more and more wells cannot form blocks singly.

Consider a well and its four adjoining background cells at $t=0$. Denote the well's temperature by $\tilde{t}_0$ and its neighbor's temperatures by $\tilde{t}_i; i=1,2,3,4$. According to the discussion in Secs. III and IV, it can be inferred that the domain wall around this single well cannot exist in some cases. If ratios between $|\tilde{t}_0|$ and $|\tilde{t}_i-\tilde{t}_0|; i=1,2,3,4$ are not large enough, the domain wall around this single well cannot exist [see Eq. (26)]. Then this well cannot be regarded as a block. It must form a block with other well. Therefore some blocks should include two wells, or more wells. As Δ decrease the probability of such wells increases. The average size of blocks b increases as Δ decreases. Considering the relation $\zeta=1/b$, one knows that ζ should decrease as Δ decreases. The decreasing of ζ for $\Delta=100$ and $t<0$ can also be explained by similar discussion.

Because some single wells cannot form blocks singly, we need an operational way to define blocks. At first, every well is investigated to see if a domain wall around this single well exists. If it exists, this well is a block. If not, this well cannot form a block. Second, all the left wells which cannot be a block singly are investigated if a domain wall around two such near wells exist. If it exists, these two near wells form a block. In similar way, we can define blocks as the average block size becomes large for lower temperature. Of course there are exceptional cases for this method, but it should be able to define most blocks because the block sizes differ not much.

For $\Delta \leq 1$, the classification is somewhat complicated. As pointed out in the previous work,[20,21] the solutions can be described by the coarse-grained approximation, in which the lattice is divided into blocks with the size n^2. In the new lattice, each cell has a local temperature $t+\tilde{t}_j^{(n)}$, where

$$\tilde{t}_j^{(n)} = \frac{1}{n} \sum_{i=(j-1)n^d+1}^{n^2 j} \tilde{t}_i. \tag{44}$$

A cell is a well if its temperature is $t+\tilde{t}_j^{(n)}<0$ and lower than its four nearest neighbors. In Fig. 13(d), the curves are the overlapping of domain wall of seven excited states for $\Delta=1$, $t=0.0$. The squares in black solid line are wells defined above with $n=4$. Because for $\Delta=1$, the proximity effect is strong, the correlation length of the ground-state solution ξ_g is about 4.[21] Therefore we take $n=4$. The domain walls are located almost in background and surround the wells. The overlapping of the domain walls of excited states divides the system into blocks clearly. According to coarse-grained approximation the solutions for $\Delta<1$ can be mapped to $\Delta=1$. The blocks can also be obtained using the above way with $n=4\Delta^{-1}$. Therefore we can still use block model to describe the excited states for the weakly disordered cases.

Through the numerical result, we see clearly how the disordered systems crossover to the pure systems. At low temperature, $t/\Delta<-1$, the number of wells does not increase remarkably. For a well, the temperature differences between it and its neighbored background cell are constants. However the ratios between the differences and the temperature of well become smaller and smaller as temperature decreases. Then the domain walls with small radius of curvature will disappear [see Eq. (26)]. Therefore as the temperature t decreases, the domain wall will become smoother and smoother, straighter and straighter, just as the situation for the well lattice in Sec. III. As $-t/\Delta \to \infty$, the domain wall should have infinite radius of curvature, just like a pure system.

C. Phase transition on the level of saddle point solution

According to the discussion similar to that in Sec. III, we get that the partition function is approximately given by the block model [Eq. (36)]. The blocks are randomly located spatially, so even the nearest-neighbored blocks are not easily defined. To be well defined, we assume that there is a coupling between two blocks only if their distance is less than $1/\zeta$, which is average distance between adjoining blocks. So the summation in Eqs. (35) and (36) is well defined. Then if we solve enough excited states, we can solve the couplings assuming the excited-state free energy is approximately given by Eq. (35). If more accurate results are wanted, it can be assumed that there is a coupling between two blocks if their distance is less than a larger cutoff than $1/\zeta$. In principle such an Ising model can be defined.

If the phase transition takes place in inhomogeneous regime, it is percolative and inhomogeneous. As we know, the coupling is weak if the background cells between two adjoining wells have positive temperature; and it is strong if the background has negative temperature. One can deal the couplings in a simple way: if the background cells have positive temperature the coupling is zero and if the background cells have positive temperature the coupling is finite. So one can only consider the clusters on which wells are connected with background with negative temperature. As temperature decreases, an infinitely large cluster composed of cells with negative temperatures should appear. As we know, this cluster is fractal. On this cluster, if the couplings between wells are strong enough, the long-range order may be realized. This percolative phase transition has been discussed by many authors.[12,25–28] A typical example of this kind of phase transition is the superconductivity transition in the granular superconductor.[25–27]

The condition of this inhomogeneous phase transition is discussed qualitatively in Ref. 21. Now based on the numerical results, we can estimate the couplings on the infinitely large cluster. At first we discuss the percolation of cells at which the ground-state solution is finite. Then we discuss the percolative phase transition on the infinitely large cluster.

For the strongly disordered cases, $\Delta \gg 1$, the probability of cells with negative temperature is 0.5, which is the site percolation threshold on square lattice. Therefore at $t=0$, an infinitely large cluster of cells with negative appears. At this temperature, it has $f_d \approx 0.09\Delta^{3/2}$ as shown in Fig. 12. Moreover at this temperature, it has $\phi_{av}/\delta_\phi \approx 1$. That is to say at percolation critical it has $\phi_{av}/\delta_\phi \approx 1$.

For $\Delta \leq 1$, the proximity effect is strong. Using the temperature to judge the amplitude of the saddle point solution is not good. We adopt $\phi_{av}/\delta_\phi \approx 1$ as the criterion of percolation critical, which is satisfied for $\Delta \gg 1$. The temperature for $\phi_{av}/\delta_\phi \approx 1$ is $t \approx 0.26$ for $\Delta=1.0$ as shown in Fig. 12. At this temperature $f_d=0.004$.

Therefore near the percolation critical, the couplings on the percolation cluster are approximately given by

$$J_{i,j} \sim g^{-1}l^{-2}bf_d \sim \begin{cases} 0.09 \times l^{d-1}\Delta_0^{3/2}/g, & l^2\Delta_0 \gg 1 \\ 0.004 \times l^d\Delta_0^2/g, & l^2\Delta_0 \leq 1. \end{cases} \tag{45}$$

where g, l, Δ_0 are the original parameters and transformation Eq. (5) is used. The fact is considered that the length of segment of domain wall between two adjoining blocks is approximately equal to the block size b. Obviously only if $J_{i,j}$ are large enough the percolative phase transition can take place.

In the homogeneous regime the couplings between a couple of adjoining blocks are also homogeneous. The temperatures in the background cells between all couples of blocks are almost negative. The local free energy increases per unit length of domain wall are almost uniform and equal to $f_d=2\sqrt{2}(-t)^{-3/2}/3$. This is valid for both of strongly and weakly disordered cases as shown in Fig. 12. However the couplings are still different since the lengths of domain wall between couples of adjoining blocks are different. The differences are not as large as those in the inhomogeneous regime. The order of couplings in homogeneous regime is given by

$$J_{i,j} \sim g^{-1}l^{-2}\zeta^{-1}f_d, \tag{46}$$

where g,l are the original parameters and transformation Eq. (5) is used. For $\Delta \gg 1$, it has $2.0 < 1/\zeta < 5.0$ in the temperature range $-4 < t/\Delta < 0$ approximately as shown in Fig. 10, and $f_d=2\sqrt{2}(-l^2t)^{3/2}/3$, where t is the original parameter. For $\Delta \leq 1.0$, it has $1/\zeta \approx 16/\Delta$ approximately as shown in Fig. 11, and $f_d=2\sqrt{2}[-l^2(t-\Delta^2 s_\Delta)]^{3/2}/3$, where t is the original parameter.

As we know, the percolative phase transition had been observed in disordered superconductors early.[25–27] From the Eq. (45), one can see why the percolative phase transition in disordered superconductors is very remarkable. For the conventional superconductor the critical region is too small to be observable in the experiments. This means, the Ginzburg-Levanyuk parameter $g^{2/(4-d)}$ is very small.[29] Therefore the coupling constant g is very small. This leads strong couplings between blocks on the percolation cluster.

The phase transition in Diluted Ising model should not be inhomogeneous. Consider that the spin occupation is p. For small $1-p$, it is far away from the percolation, and the disorder is weak. Then the LGW Hamiltonian is proper. If the diluted Ising model is mapped to the LGW Hamiltonian with random temperature, it is shown that the cell size is $l=1$ and the disorder strength is $\Delta_0=\sqrt{p(1-p)}$.[20] It belongs to the weakly disordered class $l^2\Delta_0 \leq 1$. If the Ising model without disorder is mapped to the LGW Hamiltonian using Hubbard-Statonovich transformation,[30,31] the coupling constant g equals to 1/3. Therefore the couplings on the infinitely large cluster is about $0.012p(1-p)$. The couplings is too weak to maintain a long-range order on an fractal cluster since for the pure Ising model on a square lattice the critical coupling is about 0.44.

It should take place in homogeneous regime. For $p=0.9,0.8$, the block sizes are about 53 and 40, respectively. The estimated transition temperatures are about $t_c/\Delta^2 - s_\Delta \approx -0.35, -0.28$, respectively, if $J_{i,j}/2 \approx 0.44$ (the critical coupling of pure Ising model on a square lattice) is required. These temperatures are in homogeneous regime indeed (see Fig. 8).

VI. SUMMARY AND DISCUSSION

I have carried out the numerical solution of the two-dimensional SPE of LGW Hamiltonian with random temperature. The main result is that the phase transition on the level of saddle point solutions is approximately equal to a block model, in which the blocks behave like superspins coupled with random bonds.

This result has three important consequences:

(1) Unlike pure system, there are fluctuations (of superspins) on the saddle point level for disordered systems. To distinguish fluctuation of superspins from the critical fluctuation, which is the thermodynamic fluctuation around the saddle point solution, we can call it saddle point fluctuation.

(2) Many characterizing length scales should emerge in the phase transition due to the disorder. If the network of superspins is coarse-grained again, one will get a LGW Hamiltonian with random temperature again in a larger length scale. Then on the saddle point level, one will get a block model again. This procedure can be applied again and again. In every step, one get a new and larger characterizing length scale.

(3) There may be two classes of phase transition: percolative and homogeneous. If the couplings between superspins are strong enough in inhomogeneous regime, the phase transition is percolative. Otherwise it is homogeneous.

Although our numerical solution is carried out in two dimensions, it can be expected that all above qualitative properties should be maintained in three dimensions. The scaling relations for the domain-wall length and free energy can be easily obtained.

Based on our results we can calculate the size of LOR in the experiments of disordered magnets. Grigoriev *et al.* studied the magnetic phase transition in disordered Fe-Ni alloys doped with carbon.[4–6] The size of LOR depends on the doping concentration p in the following way $R_0 \sim [p(1-p)]^{-1}$.[22] However the present experimental data is not enough to test this prediction.

There exists some evidence in favor of our block model in Monte Carlo simulation. The phenomenological argument that disordered systems are composed of compact clusters of spins, and then these clusters behave like superspins coupled to each other, was proposed early to explain Monte Carlo simulation on diluted Ising model.[32] This physical picture is explicitly shown in our work.

The phase transition in disordered systems is a complicated problem. Even for the simplest case, the two-dimensional disordered Ising model, there is a debating up to now.[33–40] There are two scenarios. The strong universality hypothesis maintains that the leading critical exponents remain the same as in the pure case and that the disorder in-

duces multiplicative logarithmic corrections to scaling, while the weak universality hypothesis favors dilution-dependent leading critical exponents. However the discrepancy and unconformity may be explained by the existence and substantial width of crossover regions. Multi characterizing length scale as mentioned above may give an explanation for the wide crossover regions.

Viewed from our result, all the RG with replica trick are problematic. In the earliest RG works done by Lubensky *et al.*, it is assumed that the saddle point solution is zero above the critical temperature.[13,14] Although these theories agree with Monte Carlo simulations for the weakly diluted Ising model, there exist substantial width of crossover regions. Most importantly, in the replicated Hamiltonian the spatial inhomogeneity disappears. Using this kind of Hamiltonian, one cannot discuss LOR, which is observed in experiments. In the later replica symmetry-breaking approach, developed by Dotsenko *et al.*, the effect of LOR is taken into account.[11] However in their conjectured saddle point solution, it is assumed that there is no coupling between LOR. Then there is no phase transition at the level of saddle point solution and the phase transition is driven by critical fluctuation. In our result there is a phase transition at the level of saddle point solution.

However the results of RG with replica agree with the Monte Carlo simulation for weakly disorder.[41–45] A possible explanation is that the conventional RG theory gives the correct asymptotic behavior but missed the correction due to the characterizing length scale emerging in the saddle point solution in this paper. As the correlation length of critical fluctuation approaches infinity, all the finite length scales play no role. In other words the saddle point fluctuation in our work may introduce modification in the intermediate length scale. This kind of modification may be not so important in the asymptotic regime, but very important in the crossover regime. For example, LOR is needed to explain experiments in doped ferromagnets.[4–6]

In addition the inhomogeneous phase has been extensively studied in various quantum phase transition in disordered systems. For example, it is found that there are two kinds of Mott transition: homogeneous and inhomogeneous.[46,47] The inhomogeneous superconducting state is also intensively studied for high-T_c superconductors.[48–51] A local metallic state is discovered in globally insulating $La_{1.24}Sr_{1.76}Mn_2O_7$ well above the metal-insulator transition.[52] From the view point of phase transition, these quantum phase transitions have been studied using RG with replica trick.[53] The saddle point solutions in these works should be solved again as in this work. It is well known that the quantum phase transition in disordered systems is a hard problem.[54] Therefore our result may shed some light on this difficult and complicated field.

ACKNOWLEDGMENTS

The author would like to thank Wenan Guo for his kind help in writing the parallel program. The author also thanks the SGI in Department of Physics in Beijing Normal University for supplying computing time. This work is supported by the Scientific Research Foundation for the Returned Overseas Chinese Scholars, State Education Ministry.

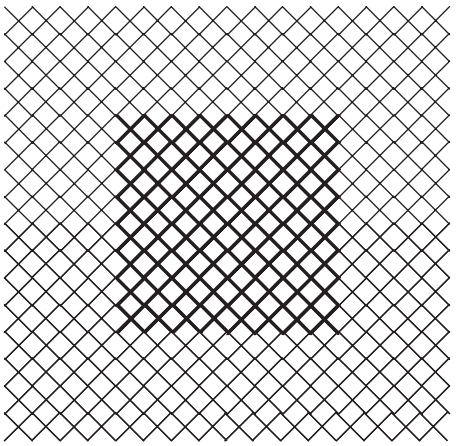

FIG. 14. The cell of spin superlattice with size being $16\sqrt{2}\times 16\sqrt{2}$. Thick bonds are J_1 and thin bonds are J_2.

APPENDIX A: A SUPERLATTICE ISING MODEL

Here we give an Ising model with the temperature field defined by Eq. (27). Consider a spin superlattice, in which each cell has $2l\times 2l$ spins. An example of such cell is shown in Fig. 14 with $l=8\sqrt{2}$. The couplings between spins are different, thick bonds are J_1, thin bonds are J_2. If $l\gg 1$, local critical temperatures for regions with J_1 and J_2 can be defined. For the spins coupled with J_1 and J_2, the local critical temperatures are $T_{c1}\approx 2.27J_1$ and $T_{c2}\approx 2.27J_2$, respectively, where the critical coupling for the Ising model on a square lattice is used. Then the reduced temperature for regions with J_1 and J_2 is approximately given by $t_1=(T-2.27J_1)/2.27J_1$ and $t_2=(T-2.27J_2)/2.27J_2$, respectively. If $J_1>J_2$, it has $t_1<t_2$. The region with J_1 is well and J_2 is background. If $(J_1-J_2)/J_1\ll 1$, it has $|t_1-t_2|\approx(J_1-J_2)/J_1$. If the size of cell $2\sqrt{2}l\times 2\sqrt{2}l$ is rescaled to be 2×2, we get $t_{bw}=|t_1'-t_2'|=l^2(J_1-J_2)/J_1$, where the transformation Eq. (5) is used. For example, if $l=20\sqrt{2}$ and $(J_1-J_2)/J_1=0.05$, it has $t_{bw}=40$.

APPENDIX B

Here we argue that the exceeding "BW" excited states discussed in Sec. V are not important.

At first, different signs at wells must have corresponding excited states, while many sets of signs at background blocks have no corresponding excited states. For example, there is no excited state in which only the sign at background block 3, as shown in Fig. 4(b), is opposite to that at other blocks. That set of signs means a closed domain wall around the background block 3 and such an excited-state solution is impossible, since only a well can resist the shrinking of domain wall.

Let us consider the excited states concerned with well 1, 2 as shown in Fig. 3(b). Assume that the signs at other wells are positive. There are four excited states: (1) $\sigma_1=-,\sigma_2=\sigma_3=+$, which is a domain wall around well 1;

(2) $\sigma_1=\sigma_3=+,\sigma_2=-$, which is a domain wall around well 2; (3) $\sigma_1=\sigma_2=\sigma_3=-$, which is state **2**A in Fig. 3(b); (4) $\sigma_1=\sigma_2=-,\sigma_3=+$, which is state **2**B in Fig. 3(b). State **2**B is only one missed in the "AE" solutions.

Second, the temperature range of existence is narrow for the exceeding "BW" states. For example, 2B as shown in the lower part of Fig. 3(b), there are two segments of domain wall crossing background block 3. Their temperature range of existence is narrow because of the interaction between the two segments of domain wall in on background block. In fact, only very few configurations with two segments crossing one background block need to be considered. Consider four wells forming a square, for example, the wells 1 and 2 and the two wells just below in the upper part of Fig. 4. We can imagine an excited state with a domain wall around the wells 1 and 2 and a same domain wall around the two wells just below. However we cannot find such an excited-state solution in numerical calculation. The reason should be that the interaction between two domain walls is too strong to allow this state to exist.

Other more complicated configurations can be similarly discussed. It seems plausible to assume that these constrained degrees of freedom do not alter the number of excited states significantly.

[1] R. B. Griffiths, Phys. Rev. Lett. **23**, 17 (1969).
[2] D. Belitz, T. R. Kirkpatrick, and Thomas Vojta, Rev. Mod. Phys. **77**, 579 (2005).
[3] S. L. Ginzburg, Zh. Eksp. Teor. Fiz. **73**, 1961 (1977) [Sov. Phys. JETP **46**, 1029 (1970)].
[4] S. V. Grigoriev, S. V. Maleyev, A. I. Okorokov, and V. V. Runov, Phys. Rev. B **58**, 3206 (1998).
[5] S. V. Grigoriev, S. A. Klimko, W. H. Kraan, S. V. Maleyev, A. I. Okorokov, M. Th. Rekveldt, and V. V. Runov, Phys. Rev. B **64**, 094426 (2001).
[6] S. V. Grigoriev, S. V. Maleyev, A. I. Okorokov, H. Eckerlebe, and N. H. van Dijk, Phys. Rev. B **69**, 134417 (2004).
[7] H. R. Glyde, O. Plantevin, B. Fåk, G. Coddens, P. S. Danielson, and H. Schober, Phys. Rev. Lett. **84**, 2646 (2000).
[8] O. Plantevin, H. R. Glyde, B. Fåk, J. Bossy, F. Albergamo, N. Mulders, and H. Schober, Phys. Rev. B **65**, 224505 (2002).
[9] V. Galitski, Phys. Rev. B **77**, 100502(R) (2008).
[10] R. M. Eremina, I. V. Yatsyk, Ya. M. Mukovskii, H.-A. Krug von Nidda, and A. Loidl, JETP Lett. **85**, 51 (2007).
[11] V. Dotsenko, A. B. Harries, D. Sherrington, and R. B. Stinchombe, J. Phys. A **28**, 3093 (1995).
[12] A. L. Korzhenevskii, H.-O. Heuer, and K. Herrmanns, J. Phys. A **31**, 927 (1998).
[13] T. C. Lubensky, Phys. Rev. B **11**, 3573 (1975).
[14] G. Grinstein and A. Luther, Phys. Rev. B **13**, 1329 (1976).
[15] A. B. Harris, J. Phys. C **7**, 1671 (1974).
[16] A. Weinrib and B. I. Halperin, Phys. Rev. B **27**, 413 (1983).
[17] V. S. Dotsenko and D. E. Feldman, J. Phys. A **28**, 5183 (1995).
[18] X. Wu, Physica **251**, 309 (1998).
[19] A. A. Fedorenko, J. Phys. A **36**, 1239 (2003).
[20] X. T. Wu and K. Yamada, J. Phys. A **37**, 3363 (2004).
[21] X. T. Wu, Phys. Rev. B **71**, 174204 (2005).
[22] X. Wu, Physica A **383**, 209 (2007).
[23] H. Schmidt and F. Schwabl, Z. Phys. B **30**, 197 (1978).
[24] S. E. Koonin, *Computational Physics* (Benjamin Cummins, California, 1986).
[25] G. Deutscher, O. Entin-Wohlman, S. Fishman, and Y. Shapira, Phys. Rev. B **21**, 5041 (1980).
[26] E. Simanek, Phys. Rev. B **25**, 237 (1982).
[27] P. L. Leath and W. Tang, Phys. Rev. B **39**, 6485 (1989).
[28] J. Rosenblatt, Phys. Rev. B **28**, 5316 (1983).
[29] L. D. Landau and E. M. Lifshitz, *Statistical Physics*, 3rd ed. (Butterworth, Washington, 1999), Vol. 1.
[30] J. Hubbard, Phys. Rev. Lett. **3**, 77 (1959).
[31] R. L. Stratonovich, Dokl. Akad. Nauk SSSR **115**, 1097 (1957); Sov. Phys. Solid State **2**, 1824 (1958).
[32] H.-O. Heuer, Europhys. Lett. **16**, 503 (1991); J. Phys. A **26**, L341 (1993).
[33] R. Kenna and J. J. Ruiz-Lorenzo, Phys. Rev. E **78**, 031134 (2008).
[34] B. N. Shalaev, Sov. Phys. Solid State **26**, 1811 (1984); Phys. Rep. **237**, 129 (1994).
[35] R. Shankar, Phys. Rev. Lett. **58**, 2466 (1987); **61**, 2390 (1988); A. W. W. Ludwig, *ibid.* **61**, 2388 (1988).
[36] G. Jug and B. N. Shalaev, Phys. Rev. B **54**, 3442 (1996).
[37] Vik. S. Dotsenko and Vl. S. Dotsenko, JETP Lett. **33**, 37 (1981); Adv. Phys. **32**, 129 (1983).
[38] J.-K. Kim and A. Patrascioiu, Phys. Rev. Lett. **72**, 2785 (1994).
[39] R. Kühn, Phys. Rev. Lett. **73**, 2268 (1994).
[40] M. Fähnle, T. Holey, and J. Eckert, J. Magn. Magn. Mater. **104-107**, 195 (1992).
[41] R. Folk, Yu. Holovatch, and T. Yavorskii, JETP Lett. **69**, 747 (1999).
[42] R. Folk, Yu. Holovatch, and T. Yavorskii, Phys. Rev. B **61**, 15114 (2000).
[43] P. Calabrese, V. Martin-Mayor, A. Pelissetto, and E. Vicari, Phys. Rev. E **68**, 036136 (2003).
[44] A. K. Murtazaev, I. K. Kamilov, and A. B. Babaev, J. Magn. Magn. Mater. **300**, e538 (2006).
[45] V. V. Prudnikov, P. V. Prudnikov, A. N. Vakilov and A. S. Krinitsyn, J. Exp. Theor. Phys. **105**, 371 (2007).
[46] D. H. Lee, J. Low Temp. Phys. **131**, 181 (2003).
[47] Y. Kohsaka, K. Iwaya, S. Satow, T. Hanaguri, M. Azuma, M. Takano, and H. Takagi, Phys. Rev. Lett. **93**, 097004 (2004).
[48] W. A. Atkinson, Phys. Rev. B **71**, 024516 (2005).
[49] A. M. Bobkov and I. V. Bobkova, Phys. Rev. B **78**, 024507 (2008).
[50] Z. Wang, J. R. Engelbrecht, S. Wang, H. Ding, and S. H. Pan, Phys. Rev. B **65**, 064509 (2002).
[51] E. V. L. de Mello, E. S. Caixeiro, and J. L. Gonzalez, Phys. Rev. B **67**, 024502 (2003).
[52] Z. Sun, J. F. Douglas, A. V. Fedorov, Y.-D. Chuang, H. Zheng, J. F. Mitchell, and D. S. Dessau, Nat. Phys. **3**, 248 (2007).
[53] D. Belitz and T. R. Kirkpatrick, Rev. Mod. Phys. **66**, 261 (1994).
[54] S. Sachdev, *Quantm Phase Transition* (Cambridge University Press, Cambridge, 1999).